

# Image Enhancement of X-ray Phase Contrast Images of Micro Objects

Application to the detection of small components in threat objects

Ivan S. Uroukov <sup>\*1</sup>, Robert Speller <sup>2</sup>, and Alessandro Olivo <sup>2</sup>

1-MRC - University of Glasgow Centre for Virus Research. 8 Church Str., Glasgow, G11 5JR., Scotland, UK.

Tel.: +44-141-330-2989. Fax: +44-141-330-3520.

2-Department of Medical Physics and Bioengineering, Malet Place Engineering Building, University College London, Gower Street, London, U.K. WC1E 6BT.

Tel.: +44 20 7679 0200 Fax: +44 20 7679 0255

\* Correspondent author. He is a former member of R. Speller's group at UCL.

<sup>1</sup>ivan.roukov@glasgow.ac.uk; <sup>2</sup>r.speller@ucl.ac.uk; <sup>2</sup>a.olivo@ucl.ac.uk

## Abstract

In x-ray based baggage scanning, the ability to identify small devices (e.g. detonator components) and explosives in baggage or shipped parcels relies on being able to characterize the materials and details that make up an x-ray image. Recently, an improvement over existing baggage scanning techniques has been proposed in the form of a system employing x-ray phase contrast imaging, as this was shown to detect smaller/fainter features and to be more sensitive to materials textures (small-scale inhomogeneities, etc).

This paper deals with additional image processing performed on the phase contrast images produced by the above system, to further improve its potential. It uses textural analysis to enhance imaged micro-structures and devices, and it has been found to be able to provide a contrast increase of up to 300% on a series of images of a phantom mimicking the presence of an explosive device plus detonator components.

## Keywords

*X-ray Imaging; Phase Contrast Imaging; Weapon Detection; Micro Objects Detection; Scanning; Gabor Filters; Intelligent Imaging*

## Introduction

X-ray phase contrast imaging (XPCI) is a novel imaging method that, by exploiting a different physical principle i.e. refraction/interference instead of attenuation, substantially enhances the sensitivity of x-ray imaging (Davis et al 1995, Snigirev et al 1995). While initially the technique was considered restricted to synchrotrons or at the very least micro focal sources, more recently methods have emerged that enable its implementation with conventional x-ray

tubes (Pfeiffer et al, 2006, Olivo and Speller 2007). This opens the way to applications in a variety of areas; among these, improved detection of threat objects was recently demonstrated in security scanning (Olivo et al, 2011, Ignatyev et al, 2011a,b).

Phase contrast X-ray imaged micro-objects are generally characterized by a higher contrast compared to standard absorption imaging. Moreover, any inhomogeneity in the object composition (at the pixel scale) would typically show up as image contrast thus creating a texture which is well suited for analysis. Texture often offers key complementary information to more extended, pixelated signal level as it is a spatial variation of the grey level rather than of its average value. Indeed in some cases in ultrasound imaging (Mohamed et al, 2003), SAR (Holmes et al, 1984, Ulaby et al, 1986 ) or biometrics (Daugman,1993) the texture (Jain et al, 1997) can be the preferred characteristic to be analysed.

According to the work of Bela Julesz, founder of texton theory (Julesz 1962, 1981, 2010), the Human Vision System (HVS) "sees" predominantly by means of textural perception. The HVS has been found to be sensitive to the frequency, direction and orientation of the viewed elements. Directionality and repetition are represented by orientation and frequency, whilst complexity is related to texture consistency.

Marcelia (1980) and Daugman (1980,1985) arrive at similar results starting from theoretical basis, by modelling the receptive field of cells in the visual cortex by means of 2D Gabor functions. Models of 'grating' and 'bar' cells in in V1 & V2 monkeys' visual cortex were shown in Petkov et al (1997).

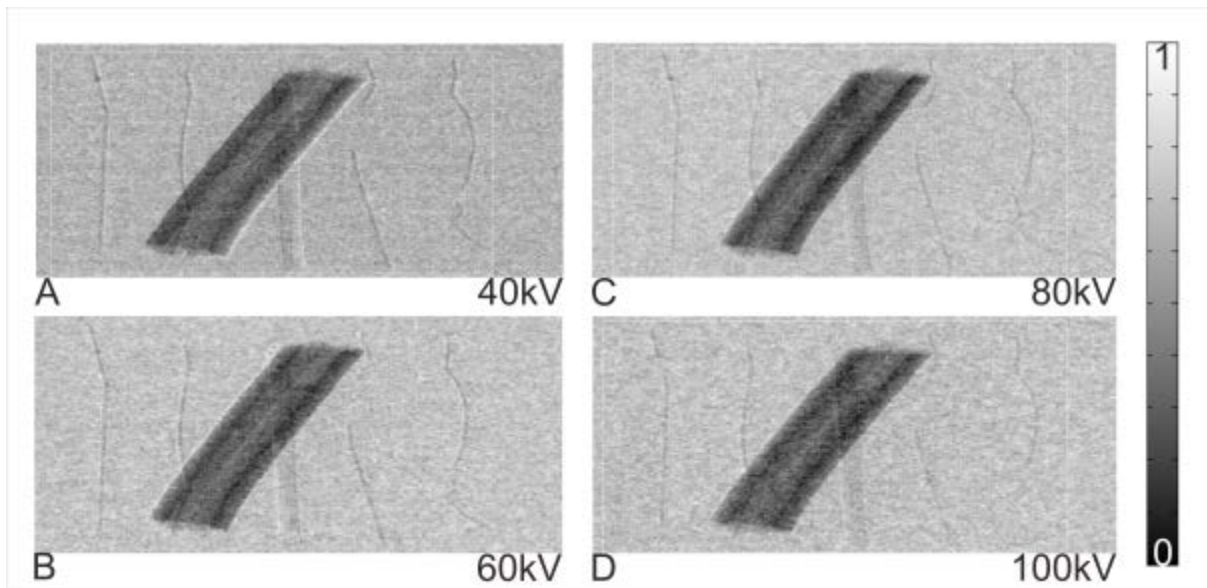


FIG. 1 X-RAY PHASE CONTRAST IMAGES OF THE CUSTOM BUILT PHANTOM SIMULATING A PLASTIC EXPLOSIVE DEVICE PLUS VARIOUS BINDING FIBRES AND THIN METALLIC WIRES (SEE TEXT). IMAGES A, B, C AND D WERE ACQUIRED AT INCREASING X-RAY TUBE VOLTAGES, AS LABELLED.

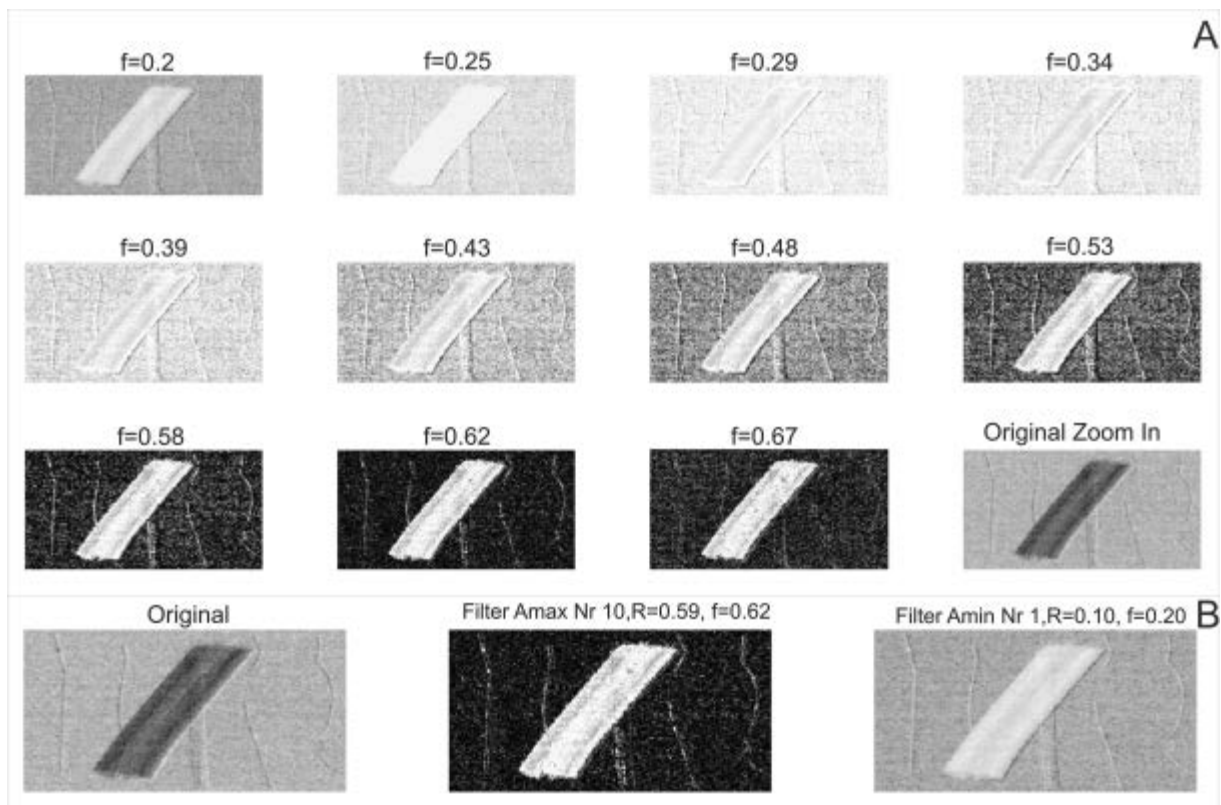


FIG. 2 A. FREQUENCY DECOMPOSITION PROCESS. AN INTEGRATION OF THE ORIENTATION DECOMPOSITION PROCESS FOR THE RANGE  $= 0 - 135^\circ$  LEADS TO SERIES OF IMAGES FOR THE RANGE OF SCANNED FREQUENCIES. IMAGES ARE LABELLED WITH THE FREQUENCY. AT SOME FREQUENCIES, THE INTENSITY RATIO BETWEEN OBJECTS (WIRES, PLASTICS) AND BACKGROUND APPROACHES 300 %. THE UNPROCESSED IMAGE IS ALSO SHOWN FOR COMPARISON (WITH THE TITLE 'ORIGINAL ZOOM IN').

B. A COMPARISON BETWEEN THE UNPROCESSED IMAGE ('ORIGINAL') AND TWO IMAGES SELECTED FROM THE RANGE OF PROCESSED ONES IS PRESENTED. WHEN THE IMAGE ENERGY IS ESTIMATED, ITS LOCAL EXTREME POINTS IDENTIFY TWO IMAGES AS MAXIMUM AND MINIMUM FOR THE SCANNED RANGE. THE IMAGE CORRESPONDING TO THIS MAXIMUM ENERGY IS ENTITLED 'FILTER AMAX NR 10, R=0.59, F=0.62'. THIS INFORMATION INCLUDES THE FILTER INDEX IN THE FILTERBANK (NR 10), THE ENERGY FACTOR R, AND THE FREQUENCY F (EXPRESSED AS REVOLUTIONS/IMAGE WIDTH). THE IMAGE AT THE MINIMUM ENERGY CONDITION IS ENTITLED WITH 'FILTER AMIN NR 1, R=0.10, F=0.20', ACCORDING TO THE SAME CATEGORIZATION CRITERIA.

In this framework by using Gabor filters optimal combined resolution can be achieved both in the spatial and frequency domain, as explained in Daugman (1985) and Jain (1991). These features has been used for image modeling in physiology and biometrics (Yunhong Wang et al., 2003), where textural features are used to generate a map of image features. This can be implemented through the ‘Iris Code’, which is based on complex valued 2D Gabor wavelets response to an image as feature descriptor (Daugman, 1993, 1994). More recently, a different software model was proposed (‘Finger Code’, Jain et al, 1999), which has 192 feature-space size, and is based on even-symmetric Gabor filter response to a fingerprint.

This work presents a novel approach to enhance the visibility of micro objects and materials imaged with XPCI through enhancing via a Gabor filterbank approach, based on textural features.

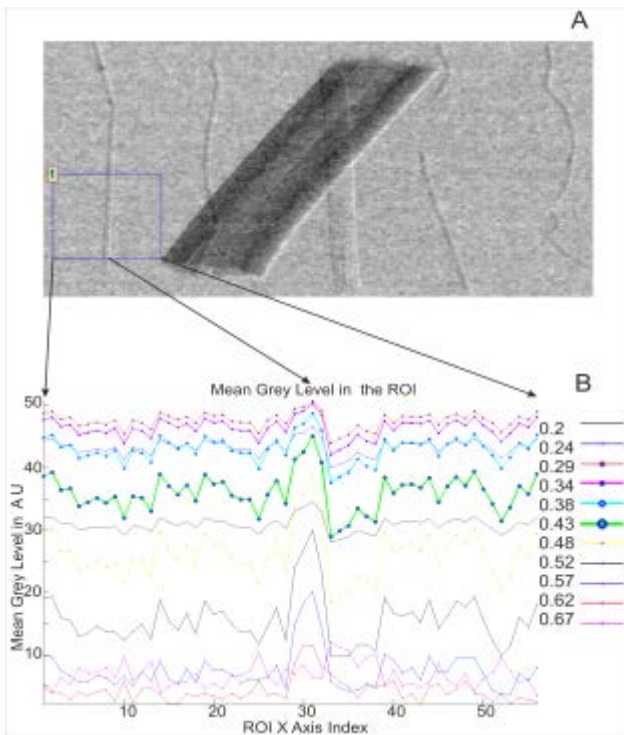


FIG. 3 MICRO WIRE PROFILES OBTAINED FOR A RANGE OF RECONSTRUCTED FREQUENCIES. SIGNAL PROFILES WERE EXTRACTED FROM A REGION OF INTEREST (ROI) AROUND A MICRO WIRE, INDICATED IN THE SQUARE LABELLED AS ‘1’ IN PANEL A. THE SIGNAL IS OBTAINED AS THE AVERAGE OVER THE LINES IN THE ROI, AND PLOTTED IN ABSOLUTE UNITS VERSUS PIXEL INDEXES ALONG THE ROI AS SHOWN IN B.

Materials and Methods

Filter Implementation

A Gabor function (Gabor, 1946) is a multi-channel

filter which has been implemented for texture analysis (Coggins, 1985). It effectively acts like a wavelet-based approach with optimal spatial and frequency identification performance, and as such can successfully isolate specific frequencies and orientations. Those features make it suitable for texture analysis. In terms of functionality, a Gabor function is a Gaussian-modulated wave. It is a product of an elliptical Gaussian with centre (X, Y) and aspect ratio  $\sigma_x/\sigma_y$ , and a complex wave (with spatial frequency  $F = \sqrt{U^2 + V^2}$  and orientation  $\theta = \tan^{-1}(V/U)$ ), which in the spatial domain can be written as:

$$f(x, y) = \frac{1}{2\pi\sigma_x\sigma_y} e^{\left(-\frac{1}{2}\left(\frac{(x-X)^2}{\sigma_x^2} + \frac{(y-Y)^2}{\sigma_y^2}\right)\right)} e^{(2\pi j[U(x-X)+V(y-Y)])}$$

eq.1

In texture research, it is widely accepted that a bank of real components of a Gabor filter can be used to characterize the channels (Jain and Farroknia, 1991). The justification for the use of an even-symmetric filter is primarily based on psychophysical grounds, but little explanation is found for this in the literature. The representation is as follow:

$$h(x, y) = \frac{1}{2\pi\sigma_x\sigma_y} e^{\left(-\frac{1}{2}\left(\frac{x^2}{\sigma_x^2} + \frac{y^2}{\sigma_y^2}\right)\right)} e^{(2\pi Fx)}$$

eq. 2

For practical purposes, the filter is presented as ‘cosine’ and ‘sine’ masks. The complete mask is obtained by point wise multiplication, and is shown below:

$$Cos.Mask(x, y) = C_N e^{\left(\frac{-r^2}{2\sigma^2}\right)} \cos(\omega x')$$

eq. 3

$$Sin.Mask(x, y) = C_N e^{\left(\frac{-r^2}{2\sigma^2}\right)} \sin(\omega x')$$

eq. 4

Where  $x' = x \cos(\theta) + y \sin(\theta)$ ,  $r^2 = x^2 + y^2$ ,  $\omega = \frac{2\pi}{T} = 2\pi f$ , and  $C_N$  is a normalization constant.

The complete mask is defined as  $Gabor.Mask = Sin.Mask * Cos.Mask$  and the filtering process effectively involves a convolution of the image with the mask, where the parameters  $\omega, \theta$  are set in advance.

X-ray Imaging

A (miniaturized) custom phantom was designed and

built to simulate the presence of a cylindrical plastic explosive plus a series of very thin ( $\sim 70 \mu\text{m}$ ) aluminium wire representing parts of the detonator system. A full description of the sample can be found in (Olivo et al, 2011) and (Ignatyev et al, 2011b). The imaging system is also described in the above papers; briefly, it consists of an X-Tek tungsten rotating target (Buckland-Wright, 1989) with a focal spot size of approximately  $30 \mu\text{m}$  full-width at half maximum (FWHM) and operated at 1 mA and 40, 60, 80 and 100 kVp (see results section). The detector is the Hamamatsu C9732DK passive-pixel CMOS flat panel, with a pixel size of 50 micron, placed at 2 m from the source. To implement the edge-illumination condition, which enables the exploitation of phase contrast effects (Olivo et al, 2001; Olivo and Speller, 2007), two x-ray masks consisting of long vertical slits carved on a gold layer electroplated on a graphite substrate (Creatv Microtech, MD) were placed one almost in contact with the detector, and the other immediately before the sample (placed midway between source and detector). The pitch and the aperture size of the slits in the detector mask were of  $100 \mu\text{m}$  and  $30 \mu\text{m}$ , respectively; covering a total area of  $6 \times 6 \text{ cm}^2$ . The pre-sample mask had the same design apart from a 50% downscaling factor accounting for the beam divergence.

### Data Processing

Images were directly saved as TIF with no compression. The images are digitised with 16-bit resolution. This resolution is computationally and optically good although the human visual system cannot distinguish more than 64 levels or  $2^5$  of grey. The algorithms were developed in Matlab, installed on a Dell Precision Workstation with 2 x Intel® Xeon® Quad Core processors with 12 GB of RAM.

### Results

Images were obtained at various X-ray tube voltages, namely 40, 60, 80 and 100 kVp as shown in figure 1 A, B, C and D, respectively. Phase effects are known to decrease more slowly with increasing energy compared to attenuation effects (Olivo et al 2011, Ignatyev et al 2011b), so this was an essential test to make sure that image (phase) contrast would still survive at the high x-ray energy levels required by security scans.

To accelerate the computational process, a portion of the image where the main objects of interest are

localised was selected. This is shown as a rectangular wire frame over images in Figure 1. From visual inspection, it is evident that the highest contrast for the micro wires is observed at 40 kVp; however, they can still be clearly detected also in the 100 kVp image. Their contrast is further enhanced through the procedure described below.

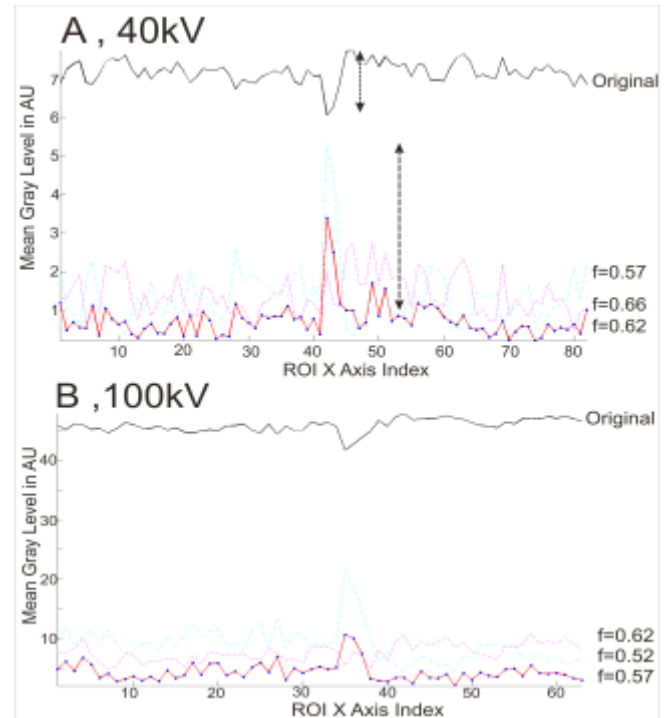


FIG. 4 A COMPARISON OF CONTRAST ENHANCEMENT IN THE SELECTED REGION OF INTEREST, FOR PROCESSED AND UNPROCESSED IMAGES, AT TWO DIFFERENT IMAGING CONDITIONS I.E. TUBE VOLTAGES OF 40 AND 100 KVP. THE PROFILES OBTAINED FROM IMAGES ARE PRESENTED FOR A RANGE OF FREQUENCIES  $f$ . THE FREQUENCY RANGE IS CENTRED AT THE MAXIMUM ENERGY IMAGE, AND VALUES ONE STEP BELOW AND ONE ABOVE IN THE FILTERBANK ( $F_{EMAX-1}, F_{EMAX}, F_{EMAX+1}$ ) ARE ALSO SHOWN. A AND B SHOW PROFILES FROM IMAGES ORIGINALLY ACQUIRED AT 40 AND 100 KVP RESPECTIVELY, AND IN BOTH CASES A CONTRAST ENHANCEMENT OF THE ORDER OF  $\sim 300\%$  IS OBSERVED.

During the computational procedure, two image decompositions are performed, one through a range of frequencies, and another through orientation, and as discussed later they are both useful for image analysis purposes. Figure 2A presents the result of this processing for the 40 kVp image, by showing the reconstructed images at a various frequencies next to the original unprocessed image for comparison

purposes. All images are labelled with the frequency of reconstruction. The image energy is measured according to Jain and Farokhnia (1991), and two local extremes (maximum and minimum) are presented in Figure 2B.

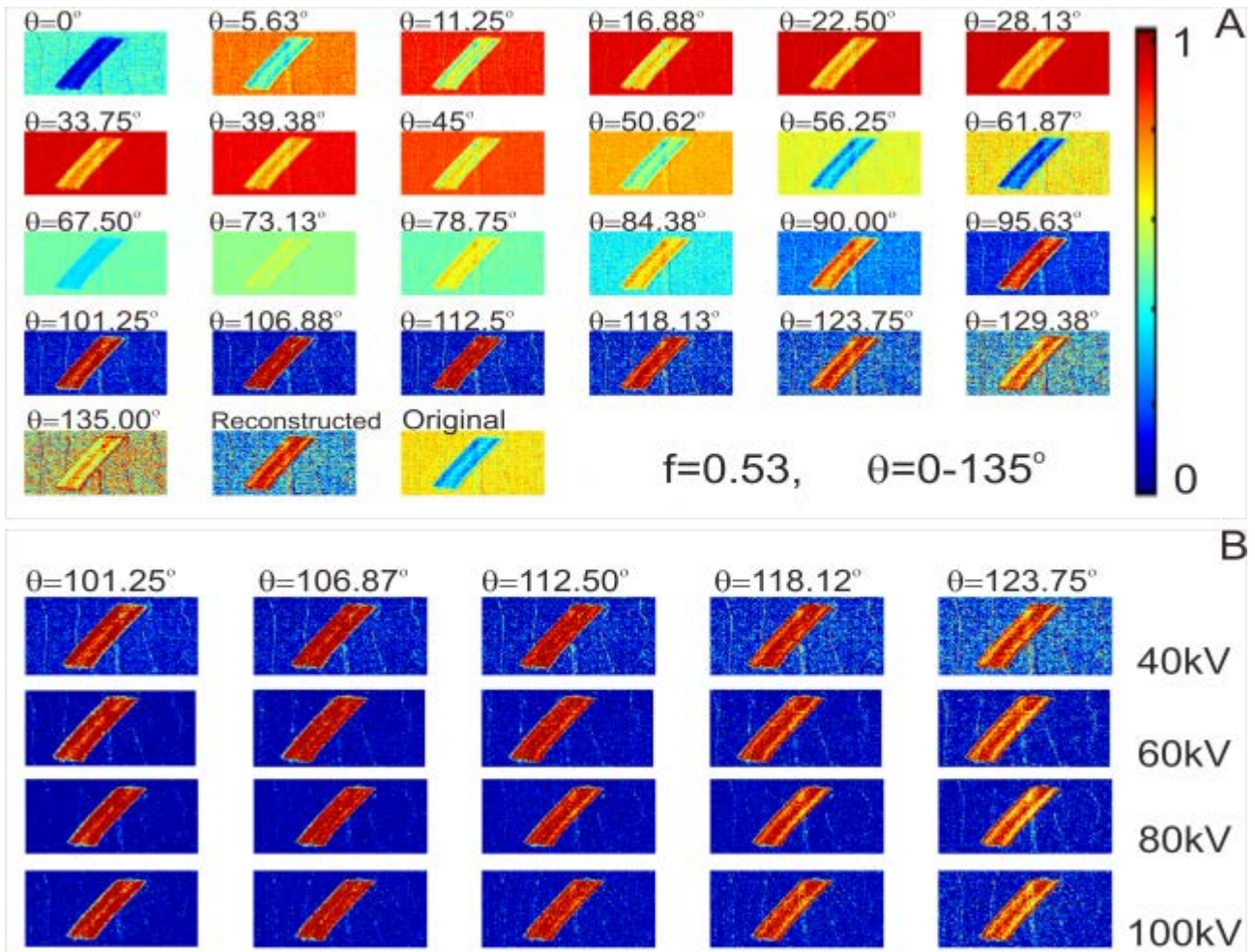


FIG. 5 A. AN EXAMPLE OF THE ORIENTATION DECOMPOSITION PROCESS WITH THE FILTERBANK (AT THE MAXIMUM ENERGY RECONSTRUCTION OBTAINED FOR  $F=0.53$ ), FOR AN IMAGE OBTAINED AT 40 KVP X-RAY TUBE VOLTAGE. THE ORIENTATION RANGE IS = 0 - 135°, WITH EACH IMAGE LABELLED ACCORDINGLY. THE RECONSTRUCTED IMAGE IS OBTAINED BY INTEGRATION OF THE SHOWN DECOMPOSED IMAGES, AND LABELLED AS 'RECONSTRUCTED'. FOR COMPARISON PURPOSES, THE UNPROCESSED IMAGE IS ALSO SHOWN IN THE SAME COLOUR MAP ('JET'). THE COLOURMAP REPRESENTS THE SIGNAL STRENGTH IN ABSOLUTE UNITS [0-1]. B. A SELECTED SUBSET OF ORIENTATION IMAGES FOR A MORE LIMITED RANGE OF VALUES IS SHOWN FOR IMAGES OBTAINED AT VARIOUS X-RAY TUBE VOLTAGES, AGAIN AT THE LOCAL MAXIMA OF THE IMAGE ENERGY MEASURE.

The image obtained at the local energy maximum is analysed further, to demonstrate the contrast enhancement that can be provided by the proposed processing method. This is done by analysing image profiles extracted from a region of interest (ROI) surrounding one of the micro wires in the image (see square labelled as "1" in figure 3A). The signals from the lines in the rectangular ROI are averaged and plotted against pixel number in Figure 3B. This shows the profile variation (over the ROI) for the entire range of images at all reconstruction frequencies, with  $f$  in the range [0.2, 0.67].

The analysis on images obtained at maximum energy is then repeated for different x-ray tube voltages, and the result is shown in Figure 4. The profiles obtained from the same ROIs of unprocessed and processed images are shown, for acquisitions performed at 40

kVp (Figure 4A) and 100 kVp (figure 4B). For comparison purposes, for the processed images, profiles are presented both for the maximum energy image and for images obtained one step below and one above in the filterbank ( $f_{Emax-1}, f_{Emax}, f_{Emax+1}$ ).

As shown in Figure 2A, frequency decomposition yields a contrast enhancement of about 300%. Each frequency reconstructed image is the result of the integration of a range of orientation-decomposed images, as shown in Figure 5A. This integration is performed at a selected frequency which corresponds to the local maximum of the image energy, as indicated in Figure 5A. Some orientation bands result in a better conspicuity of the micro wires, especially in the range of 90° - 120°. A 'jet' colour map is used for a better visualisation of the image features. Finally, an analysis of a range of images as a function of the X-ray

tube voltage is shown on Figure 5B. It demonstrates the enhanced contrast in the filter orientation range between  $101.25^\circ$  -  $121.25^\circ$ . As anticipated (and expected), the contrast is higher at 40 kVp, but all image features are still visible at 100 kVp. Most importantly, the degree of contrast improvement provided by the proposed processing technique is similar for all tube spectra and, for the selected images, is of the order of 300%.

## Conclusions

This paper combines a new imaging technique (edge-illumination XPCI) with a novel textural analysis approach, and applies it to the detection of faint features in security scanning. The XPCI method enables the generation of image contrast for small and weakly absorbing details for beam spectra of up to 100 kVp, as required in security applications; the textural processing further increases the contrast of the details of a factor up to 300%. These findings go along the lines of previous observations in Synthetic Aperture Radar (SAR) (Ulaby, 1986) or biometrics (Daugman, 1994), where either features already distinguishable were further enhanced, or even some which remained almost hidden due to low contrast were better revealed with the proposed filtering. It should be noted that, while here we have presented an application to security scans as a possible example, the method is general enough to be applied in other areas such as medicine, material science, etc.

## ACKNOWLEDGMENT

This project was funded under the Innovative Research Call in Explosives and Weapons Detection (2008) initiative, a cross-government programme sponsored by a number of government departments and agencies under the CONTEST strategy. A. Olivo is supported by the EPSRC (Grants EP/G004250/1 and EP/I021884/1).

## REFERENCES

- Buckland-Wright J. C., A new high-definition microfocal x-ray unit, *Br. J. Radiol.* 62, 201-208, 1989.
- Coggins J.M. and Jain A.K., A spatial filtering approach to texture analysis. *Pattern Recognition Letters* 3(3), 195-203, 1985.
- Daugman J.G., High confidence visual recognition of persons by test of statistical independence. *IEEE Transactions on pattern analysis and machine intelligence*, Vol. 15, No 11, November 1993.
- Daugman J.G., Two-dimensional spectral analysis of cortical receptive field profiles. *Vision Research* 20, 847-856, 1980.
- Daugman J.G., Uncertainty relation for resolution in space, spatial frequency, and orientation optimized by two-dimensional visual cortex filters. *J. Opt.Soc. Am. A.2(7)*, 1160-1169, 1985.
- Daugman John G., United States Patent, Patent Number 5,291,560, Date Mar. 1,1994.
- Davis T. J., Gao D., Gureyev T. E., Stevenson A. W. and Wilkins S. W., Phase-contrast imaging of weakly absorbing materials using hard x-rays. *Nature* 373, 595-598, 1995.
- Gabor, D., Theory of communication, *J. Inst. Elect. Ing.* 93 (1946), 429-457.
- Holmes Q.A., Nuesch D.R., and Shuchman R.A., Textural analysis and real-time classification of sea-ice types using digital SAR data. *IEEE Trans. Geosci. Remote Sensing. GE-22*, 2, 113-120, 1984.
- Ignatyev K., Munro P. R. T., Chana D., Speller R. D. and Olivo A. A new generation of x-ray baggage scanners based on a different physical principle, *Materials* 4, 1846-1860, 2011(a).
- Ignatyev K., Munro P. R. T., Chana D., Speller R. D. and Olivo A. Coded apertures allow high-energy x-ray phase contrast imaging with laboratory sources. *J. Appl. Phys.* 110, 014906, 2011(b).
- Jain A. K. and Farrokhnia F., Unsupervised texture segmentation using Gabor Filters. *Pattern Recognition* 24(12), 1167-1186, 1991.
- Jain A. K., IEEE, Prabhakar S., and Hong L., A Multichannel Approach to Fingerprint Classification, *IEEE Transaction on patterns analysis and machine intelligence*, Vol. 21, No. 4, APRIL 1999.
- Jain A.K., Ratha N.K., and Lakshmanan S., Object Detection Using Gabor Filters, *Pattern Recognition* 30(2), 295-309, 1997.
- Julesz B. A theory of preattentive texture discrimination based on first order statistics of textons., *Biol. Cybernetics*, 41:131-178,1981.
- Julesz B. Visual pattern discrimination., *IRE Trans. On information Technology*, IT-8:84-92, Feb 1962.

- Julesz Bela, Preattentive human vision: link between neurophysiology and psychophysics. Chapter 14, AT & T Bell Labs, Published in: Comprehensive Physiology, 1 Jan 2011.
- Marcelja S., Mathematical description of the responses of simple cortical cells. J. Opt. Soc. Am. 70(11), 1297-1300, 1970.
- Mohamed S. S., Abdel-galil T. K., Salama M. M. A., El-saadany E. F., and Kamel M., Fenster A., Downey D. B., and Rizkalla K., Prostate cancer diagnosis based on Gabor filter texture segmentation of ultrasound image. CCECE 2003 – CCGEI 2003.
- Olivo A. and Speller, R., A coded-aperture technique allowing x-ray phase contrast imaging with conventional sources, Appl. Phys. Lett. 91, 074106, 2007.
- Olivo A., Arfelli F., Cantatore G., Longo R., Menk R. H., Pani S., Prest M., Poropat P., Rigon L., Tromba G., Vallazza E. and Castelli E., An innovative digital imaging set-up allowing a low-dose approach to phase contrast applications in the medical field, Med. Phys. 28, 1610-1619, 2001.
- Olivo A., Ignatyev K., Munro P. R. T., and Speller R. D. Noninterferometric phase-contrast images obtained with incoherent x-ray sources", Appl. Opt. 50, 1765-1769, 2011.
- Petkov N., Kruizinga P., 1997. Computational models of visual neurons specialised in the detection of periodic and aperiodic oriented visual stimuli: bar and grating cells, Biol. Cybern., 76, 83–96.
- Pfeiffer F., Weitkamp T., Bunk O., and David C., Phase retrieval and differential phase-contrast imaging with low-brilliance x-ray sources, Nat. Phys. 2, 258-61, 2006.
- Snigirev A., Snigireva I., Kohn V., Kuznetsov S., and Schelokov I., On the possibilities of x-ray phase contrast microimaging by coherent high-energy synchrotron radiation, Rev. Sci. Instrum. 66, 5486-5492, 1995.
- Ulaby F.T., Kouyate F., Brisco B., and Williams T.H.L., Textural information in SAR images. IEEE Trans. Geosci. Remote Sensing. GE 24, 235-245, 1986.
- Yunhong Wang, Tieniu Tan, Jain A. K., Combining Face and Iris Biometrics for Identity Verification, J. Kittler and

M.S. Nixon (Eds.): AVBPA 2003, LNCS 2688, pp. 805–813, 2003. Springer-Verlag Berlin Heidelberg 2003.



**Ivan S. Uroukov** (Dipl. Eng. Physicist, MSc, PhD) is a graduate in Condensed Matter Physics from the Bulgarian Academy of Sciences, Sofia, Bulgaria. He has worked and published in semiconductor physics, biophysical imaging, image computing and biological information processing topics. He has investigated the use of these approaches for examining material science aspects of biomedical and security imaging. He is currently engaged in applying signal and image computing with psychophysical approach to ultra-low contrast imaging techniques, such as electron microscopy of unstained, frozen, biological specimens and similar imaging modalities. He also has interests in biologically inspired signal and information processing. Dr Uroukov is a member of Society for Neuroscience, USA, 2008.



**Robert Speller** is the Joel Professor of Physics Applied to Medicine at University College London. He is Head of the Radiation Physics Group. A group of ~30 members with interests in scattered radiation fields, X-ray diffraction, phase contrast imaging, radioisotope mapping, heavy charged particle radiotherapy and tomographic techniques applied to a range of problems covering medicine, security and industry. He holds patents in a range of imaging techniques including phase contrast imaging and is a Fellow of the Royal College of Radiologists.



**Alessandro Olivo** is Professor of Applied Physics at University College London. He is a pioneer in the field of phase-contrast imaging, having developed early medical applications (especially to mammography) and participated in the design of the in vivo phase contrast mammography system operational at the Elettra synchrotron in Italy. He is the inventor of the "edge-illumination" and "coded-aperture" phase contrast imaging methods, and currently runs a 9-strong group at UCL, at the centre of a large European collaboration, which aims at the further development of phase-based x-ray methods and their application to a range of interdisciplinary areas.